

# Lipophilic Analogs of Thioflavin S as Novel Amyloid-Imaging Agents

Chunying Wu<sup>1</sup>, Lisheng Cai<sup>2</sup>, Jingjun Wei<sup>1</sup>, Victor W. Pike<sup>2</sup> and Yanming Wang<sup>1,\*</sup>

<sup>1</sup>College of Pharmacy, Department of Medicinal Chemistry and Pharmacognosy, University of Illinois at Chicago, Chicago, IL 60612, USA; <sup>2</sup>Molecular Imaging Branch, National Institute of Mental Health, National Institutes of Health, 10 Center Drive, Bethesda, MD 20892, USA

**Abstract:** Lipophilic analogs of thioflavin S were synthesized and radiolabeled with positron or single photon emitting radionuclides. The binding affinity for A $\beta$  was evaluated using isolated amyloid fibrils from human brain tissue. Binding specificity was assessed using fluorescent tissue staining. *In vivo* brain uptake was evaluated in mice. Following synthesis, neutral analogs of thioflavin S capable of radiolabeling with <sup>11</sup>C or <sup>125</sup>I, were found to bind isolated human A $\beta$  with affinities in the nanomolar range. Fluorescent tissue staining showed selective binding to A $\beta$  deposits *in vitro*. Biodistribution of selected compounds displayed high brain permeability at early time points. At later points, the compounds were cleared from the normal brain, indicating low non-specific binding *in vivo*. These studies indicated that novel amyloid imaging probes can be developed based on thioflavin S that readily entered the brain and selectively bound to A $\beta$  deposits and neurofibrillary tangles. Potential applications of these amyloid binding agents include facilitating drug screening in animal models and use as *in vivo* markers of early and definitive diagnosis of AD.

**Keywords:** Amyloid- $\beta$ , Alzheimer's disease, Thioflavin S, PET, SPECT, Imaging.

## 1. INTRODUCTION

Alzheimer's disease (AD) is the leading cause of dementia among the elderly population that affects over 4 million people in the US and costs the nation 100 billion dollars each year [1-3]. To date, significant progress has been made both in understanding the disease and in the therapeutic treatments. Some of the key pathological features of AD include extracellular accumulation of amyloid- $\beta$  peptides (A $\beta$ ) forming senile plaques (SPs), and intracellular aggregation of highly phosphorylated tau proteins forming neurofibrillary tangles (NFTs) [4-7]. A $\beta$  peptides, which contain 40-42 amino acid residues, are generated by cleavage of amyloid precursor protein (APP) [8, 9]. A $\beta$  peptides tend to adopt to beta-sheet conformation and are therefore prone to aggregation into fibrillar structure. Subsequent deposition primarily occurs in the regions of the frontal cortex and hippocampus of the brain [10]. Evidence has shown that deposition of A $\beta$  aggregates initiates inflammatory response and may proceed the formation of NFTs [11, 12]. Although the exact roles of A $\beta$  deposition in AD pathogenesis are still up for debate, recent studies strongly suggest that A $\beta$  deposition is an early and specific event in the pathogenesis of AD [9, 13, 14]. This necessitates development of an imaging tool that allows for *in vivo* detection and quantitation of amyloid loads in the brain. Once developed, it can be useful in early and definitive diagnosis of AD. More importantly, it can facilitate efficacy of evaluation of anti-amyloid therapies currently under development. These anti-amyloid therapies include prevention of aggregation and deposition of amyloid- $\beta$  peptides in the brain clearance of A $\beta$  from the brain.

Toward this goal, my group and others have set out to develop amyloid imaging agents for positron emission tomography (PET) and single photon emission computed tomography (SPECT) [15]. PET and SPECT are two powerful imaging techniques, used in conjunction with trace amounts of radioligands, to non-invasively detect and quantify amyloid deposits in the brain. A key step is the development of radioligands with suitable pharmacokinetic profiles in the whole process of amyloid imaging with PET or SPECT [16-18]. Once labeled with appropriate radionuclides (i.e. <sup>18</sup>F or <sup>11</sup>C for PET and <sup>123</sup>I or <sup>99m</sup>Tc for SPECT), amyloid imaging agents should readily enter the brain and selectively bind to amyloid deposits with high affinity.

One strategy in the development of amyloid-imaging agents has been centered on neutral and lipophilic analogs of amyloid dyes that are widely used in AD pathology. The existing amyloid dyes are often charged, small molecules that are too hydrophilic to enter the brain. Over the past several years, our group and others have explored the potential to develop neutral and lipophilic analogs of amyloid dyes as amyloid-imaging agents that can be labeled with different radionuclides for PET or SPECT studies. By systematically optimizing the structures of amyloid dyes, the lipophilicity can be increased to such an extent that the so-obtained analogs can readily diffuse across the blood-brain barrier (BBB) while maintaining high binding affinity and specificity for amyloid deposits in the brain.

Accordingly, small molecule amyloid imaging agents have been developed based on Congo red (CR) and thioflavin T (ThT) [16]. Systematic modification of CR and ThT and subsequent structure activity relationship (SAR) studies led to identification of several types of potential amyloid-specific imaging agents for PET or SPECT imaging such as styrylbenzene analogs [16, 19-29], stilbene analogs [30-32] and benzothiazole analogs [20, 22, 33-39]. Derivatives of

\*Address correspondence to this author at the College of Pharmacy, Department of Medicinal Chemistry and Pharmacognosy, University of Illinois at Chicago, Chicago, IL 60612, USA; E-mail: ymwang@uic.edu

other histological dyes such as acridine orange [40, 41], fluorene [42] and DDNP [43-45] (Fig. 1) have also been explored. Among these amyloid imaging agents, three lead compounds termed PIB, FDDNP, and SB-13 have been identified and evaluated in human subjects (Fig. 2) [46]. Along these progresses, some challenges still remain. For example, amyloid-imaging agents to be developed should be capable of studies in both animal models and human subjects based on the same imaging modalities. This would allow for direct translational research in drug discovery and development. Although some lead compounds have been identified suitable for PET studies in human subjects, none of them could be used for microPET studies in animal models. In addition, PET and SPECT complement each other in terms of performance and costs. While PET provides high resolution and quantitative capacity, SPECT is still the key imaging modality in most nuclear imaging facilities. However, progress is limited in the development of lead compounds for SPECT studies.

To meet these challenges, amyloid-imaging agents with distinct *in vivo* pharmacokinetics have to be developed. This necessitates the search for new amyloid-binding pharmacophores that are different from CR and ThT. In order to develop novel amyloid imaging agents, we turned to another widely used amyloid dye, thioflavin S (ThS). To date, the potential of ThS has not been systematically explored for amyloid imaging. This is in part due to the fact that ThS exists as a mixture of at least 6 components. The structure of a major component of ThS is a charged di-benzothiazole derivative as shown in Fig. (1).

Following our previous studies [47], the lipophilicity was enhanced by eliminating the charges of ThS through removal of the methyl group on the benzothiazolium nitrogen and the

sulfonate group on the benzene ring. The increase in lipophilicity normally leads to increased brain permeability as suggested by our previous SAR studies of amyloid imaging agents [33, 35]. We then set out to develop neutral and lipophilic analogs of ThS as novel amyloid imaging agents with suitable *in vivo* pharmacokinetics profiles. Systematic modifications of ThS led us to synthesize a series of alkyl (aryl)-substituted bis-benzothiazole derivatives. These ThS analogs are more lipophilic than ThS and neutral at physiologic pH. These compounds were also designed so that they could readily be labeled with  $^{11}\text{C}$  through radiomethylation or labeled with  $^{125/123}\text{I}$  through radioiodination. In this work, the synthesis and biological evaluation of these ThS analogs are described for potential application in amyloid imaging.

## 2. RESULTS AND DISCUSSION

### 2.1. Chemical Synthesis

To date, we have designed and synthesized a series of lipophilic analogs of ThS (Table 1). Two synthetic approaches were employed, depending on the positions of functional groups and the availability of starting materials. The synthesis of compounds 4-(6-methyl-[2,6']bibenzothiazol-yl-2'-yl)-aniline (**8**) and *N*-methyl-4-(6-methyl-[2,6']bibenzothiazol-yl-2'-yl)-aniline (**9**) is shown in scheme 1. Starting from commercially available 2-amino-6-methylbenzothiazole, hydrolysis using potassium hydroxide yielded the 2-mercapto-4-methylaniline (**2**), which was then coupled with 4-nitrobenzaldehyde to afford 6-methyl-2-(4'-nitrophenyl)benzothiazole (**3**). Further reduction of the nitro group of **3** furnished 4-(6-methyl-benzothiazol-2-yl)-aniline (**4**). The amino-intermediate (**4**) was treated with KSCN and  $\text{Br}_2$  in DMF overnight to generate the aminobenzothiazole

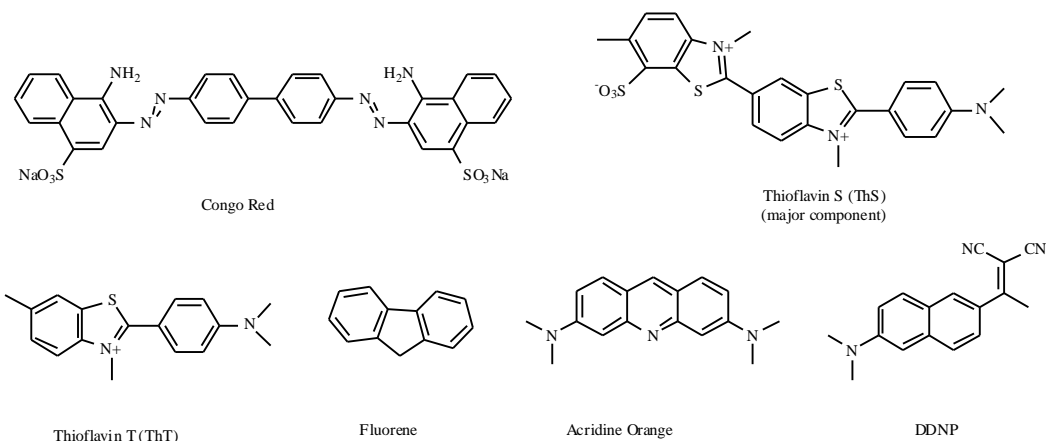


**Fig. (1).** Structures of prototypes of amyloid plaque-specific compounds

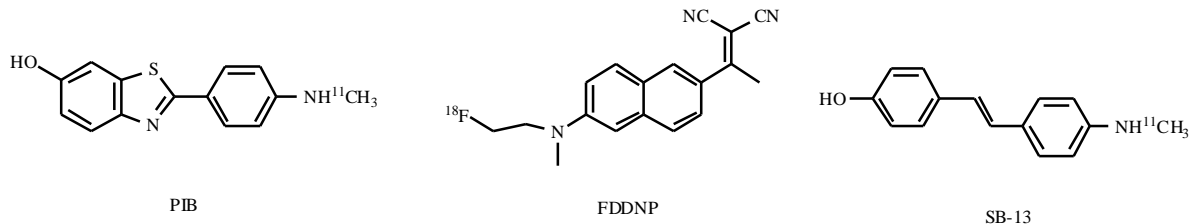
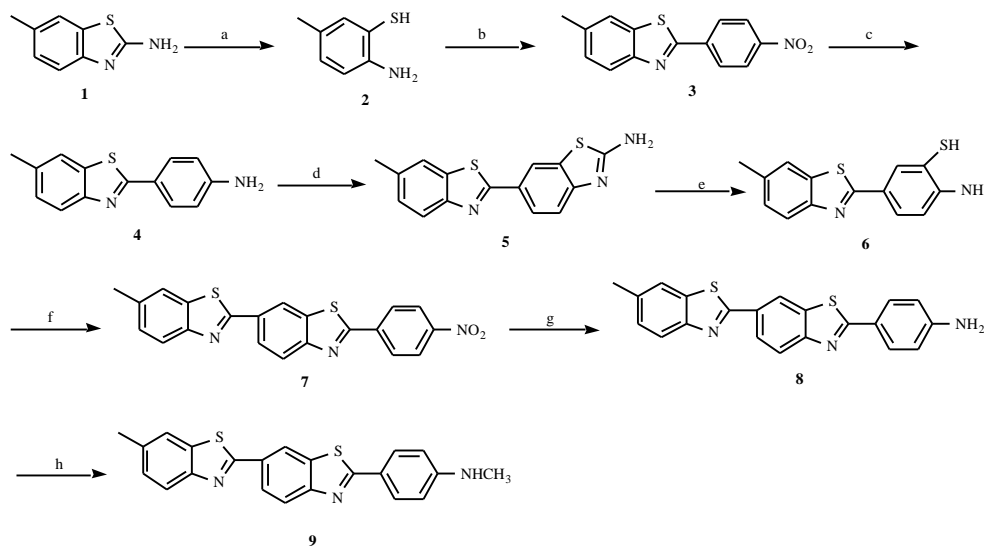


**Fig. (2).** Structures of some successful lead amyloid imaging agents that have been studied in human subjects.

Table 1. Structures of Lipophilic Analogs of ThS and their Physicochemical Properties

Compound	Structure	Postmortem tissue staining	Ki (nM)	LogP (Oct)
PIB		+	37 ± 19	1.23 <sup>a</sup>
8		+	106 ± 55	2.00 <sup>b</sup>
9		+	121 ± 48	2.60 <sup>b</sup>
[ <sup>125</sup> I]8		-	-	3.10 <sup>c</sup>
16		+	29 ± 11	1.60 <sup>b</sup>
17		+	23 ± 16	2.20 <sup>b</sup>
[ <sup>125</sup> I]16		-	-	2.70 <sup>c</sup>

a) from references [35]. b) estimated. c) experimentally determined.



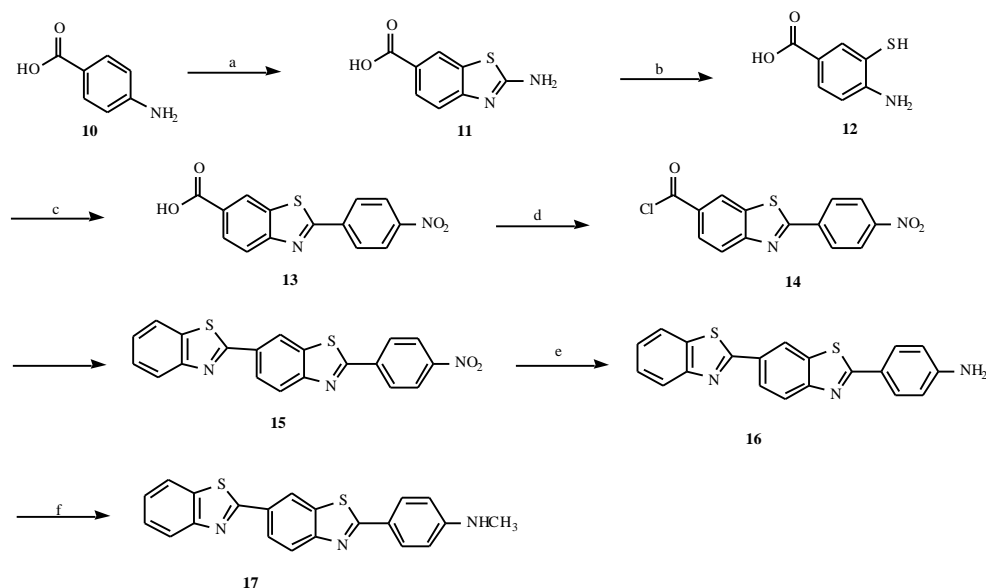
a) KOH, H<sub>2</sub>O, ethylene glycol, reflux, 2 days; b) *p*-nitrobenzaldehyde, DMSO, 170 °C, 20 min; c) SnCl<sub>2</sub>, ethanol, reflux, 4 hours; d) KSCN, Br<sub>2</sub>, DMF, overnight; e) 1. KOH, H<sub>2</sub>O, reflux 3 hours; 2. ZnCl<sub>2</sub>, 64%; f) *p*-nitrobenzoyl chloride, chlorobenzene, reflux, 3 hours, quant.; g) SnCl<sub>2</sub>, conc. HCl, 80 °C, 1 hour, 49%; h) MeI, K<sub>2</sub>CO<sub>3</sub>, 100 °C, 28 hours.

**Scheme 1.** Synthesis of compound 4-(6-methyl-[2,6']biphenyl-2'-yl)-aniline (**8**) and *N*-methyl-4-(6-methyl-[2,6']biphenyl-2'-yl)-aniline (**9**).

intermediate (**5**), which was purified by recrystallization in acetic acid [48]. Hydrolysis of **5** yielded the zinc salt of aminothiophenol **6**, which was then coupled with *p*-nitrobenzoyl chloride to give 6-methyl-2'-(4-nitro-phenyl)-[2,6']biphenyl-2-ylamine (**7**). Reduction of **7** led to the targeted compound 4-(6-methyl-[2,6']biphenyl-2'-yl)-aniline (**8**). Methylation with CH<sub>3</sub>I afforded *N*-methyl-4-(6-methyl-[2,6']biphenyl-2'-yl)-aniline (**9**).

The synthesis of 4-([2,6']biphenyl-2'-yl)-aniline (**16**) and *N*-methyl-4-([2,6']biphenyl-2'-yl)-aniline (**17**) are shown in scheme 2. Starting from the commercially available 4-aminobenzoic acid, the 2-aminobenzothiazole-6-carboxylic acid (**11**) was synthesized [48]. After hydrolyzing

the aminobenzothiazole ring of **11**, the zinc salt of the 4-amino-3-mercaptobenzoic acid (**12**), was obtained as the key intermediate. The zinc salt of **12** was then immediately coupled with *p*-nitrobenzoyl chloride to give 2-(4-nitro-phenyl)-benzothiazole-6-carboxylic acid (**13**). Using thionyl chloride as acylating reagent, compound **13** was converted into 2-(4-nitro-phenyl)-benzothiazole-6-carbonyl chloride (**14**), which was used for the coupling with 2-aminothiophenol without further purification to give 2'-(4-nitro-phenyl)-[2,6']biphenyl-2-ylamine (**15**). Reduction of **15** afforded 4-([2,6']biphenyl-2'-yl)-aniline (**16**), which was further methylated to *N*-methyl-4-([2,6']biphenyl-2'-yl)-aniline (**17**).



a) reference [48]; b) KOH, H<sub>2</sub>O, ZnCl<sub>2</sub>, 97%; c) *p*-NO<sub>2</sub>-PhCOCl, C<sub>6</sub>H<sub>5</sub>Cl, 81.5%; d) 1 : SOCl<sub>2</sub>, 2 : 2-aminothiophenol, 79%; e) SnCl<sub>2</sub>, conc. HCl, quant.; f) MeI, K<sub>2</sub>CO<sub>3</sub>, DMSO, 7%.

**Scheme 2.** Synthesis of 4-([2,6']bibenzothiazolyl-2'-yl)-aniline (**16**) and *N*-methyl-4-([2,6']bibenzothiazolyl-2'-yl)-aniline (**17**).

All the synthesized compounds were identified by <sup>1</sup>HNMR and HR-ESIMS. The detailed experimental procedures and analytical data will be published elsewhere.

## 2.2. *In Vitro* Postmortem Tissue Staining

The ThS analogs we synthesized are fluorescent compounds. The binding specificity of ThS analogs for amyloid deposits was first evaluated through fluorescent staining of postmortem AD brain tissue sections. *In vitro* tissue staining was conducted in paraffin embedded post-mortem AD brain sections. At a concentration of 10 μM, these compounds clearly stained amyloid plaques and NFTs very well (Fig. 3). While both amyloid plaques and NFTs in post-mortem brain sections of AD patients were observed, some compounds appeared to bind NFTs more intensely than amyloid plaques. The tissue staining results indicated that binding affinity for amyloid plaques and NFTs could be retained after elimination of the positive charges of ThS.

## 2.3. *In Vitro* Binding to Isolated Human Amyloid

Fluorescent tissue staining only provides qualitative assessment of binding affinity and specificity. In order to quantitatively evaluate the binding properties of these newly developed compounds, we conducted radioligand-based competitive binding assays. In this quantitatively binding assay, we used isolated AD human beta-amyloid fibrils and tritiated PIB ([<sup>3</sup>H]PIB) as radioligand, a compound known to have high affinity for synthetic A<sub>β</sub> aggregation (*K*<sub>i</sub> = 4.3 nM) [33] and has already successfully been studied on human beings. Approximately 95% of [<sup>3</sup>H]PIB binding to isolated AD amyloid was displaced by 1.0 μM unlabeled PIB. The ThS analogs compete for PIB binding site(s), indicating that they share the same binding sites as PIB. Relatively high affinities were observed for isolated human A<sub>β</sub>, some even

better than that of PIB itself. As shown in (Fig. 4), compound **16** and **17** displayed binding affinities *K*<sub>i</sub> = 29 nM and *K*<sub>i</sub> = 23 nM, respectively. In combination with the results of *in vitro* postmortem AD brain tissue staining, compound **16** and compound **17** showed promising features for mapping amyloid plaques and NFTs in AD subjects. We therefore selected these two compounds as lead compounds for further studies. In addition, compound **16** was labeled with <sup>11</sup>C at 4' position for potential use as a PET radiotracer and labeled with <sup>123/125</sup>I at 3' position for potential use as a SPECT radiotracer as discussed below.

## 2.4. Radiosynthesis

The radiosynthesis of [<sup>11</sup>C]**17** is shown in Scheme 3. For <sup>11</sup>C-labelling, radiomethylation reaction was carried out by bubbling <sup>11</sup>CH<sub>3</sub>I into the solution of compound **16** in DMSO in the presence of anhydrous KOH. The reaction mixture was then stirred at room temperature for 30 min followed by heating at 125°C for 5 min. The [<sup>11</sup>C]**17** with high specific activity (2.0 Ci/μmol) and radiochemical purity (98%) were then obtained by HPLC purification. The chemical identity of the C-11-labeled radioligands was verified by co-elution of the non-radioactive compound **17** on high performance liquid chromatography (HPLC) analysis.

The radiosynthesis of [<sup>125</sup>I]**8** and [<sup>125</sup>I]**16** were shown in Scheme 4. By using sodium [<sup>125</sup>I] iodide in the presence of chloramine T (Ch-T), [<sup>125</sup>I]**8** and [<sup>125</sup>I]**16** were prepared with radiochemical purity over 98% and a specific activity near the theoretical limit (2.1 Ci/μmol). As monitored by HPLC, the reaction went to completion after 3 h. The overall yields of [<sup>125</sup>I]**8** and [<sup>125</sup>I]**16** were 20-30% after HPLC purification. [<sup>125</sup>I]**8** and [<sup>125</sup>I]**16** were stable enough to be kept at room temperature for up to 8 h and in the refrigerator for up to 2 months.

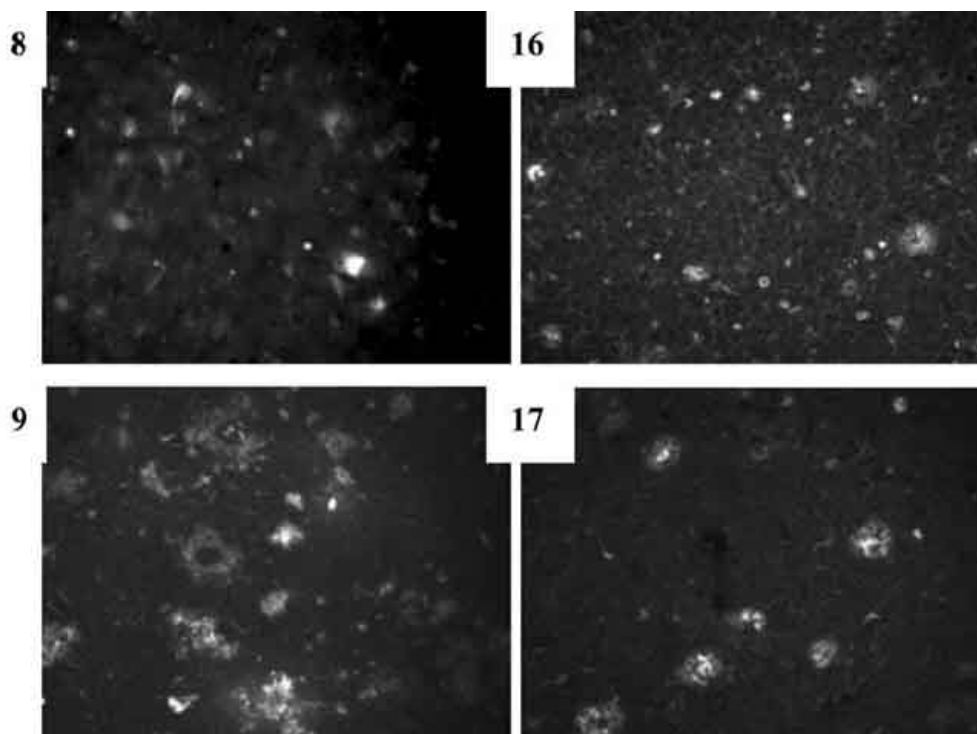


**Fig. (3).** Post-mortem brain tissue sections from AD subjects stained with 10  $\mu$ M tested compounds **8**, **9**, **16** and **17** showing selective labeling of amyloid plaques and neurofibrillary tangles.

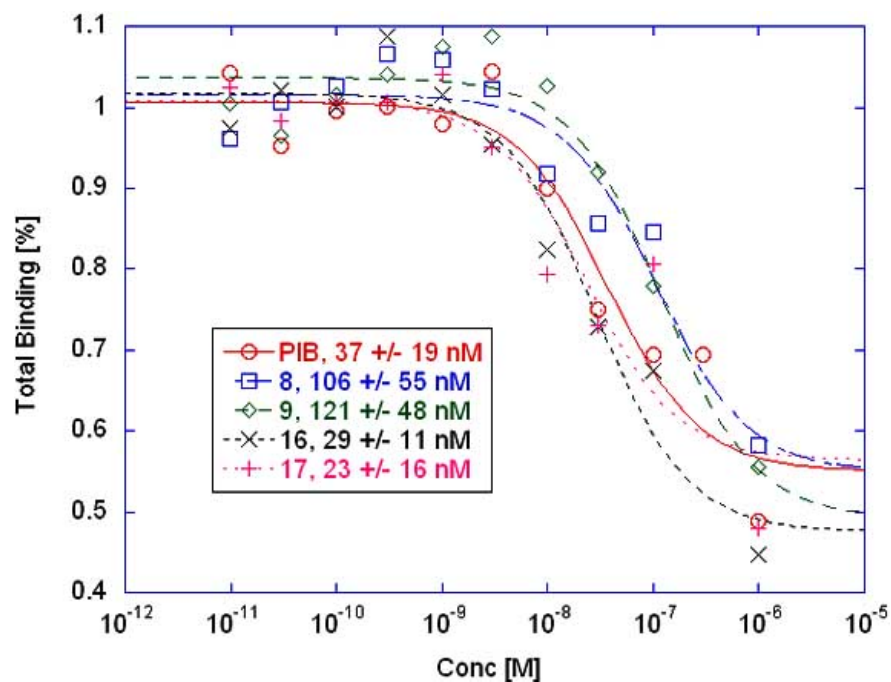
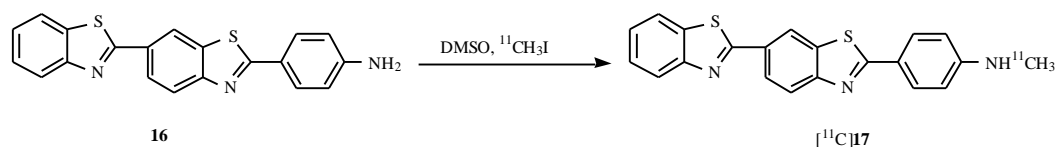


**Fig. (4).** Competitive binding assays of ThS derivatives in isolated human A $\beta$  fibrils using [ $^3$ H]PIB as the radioligand.

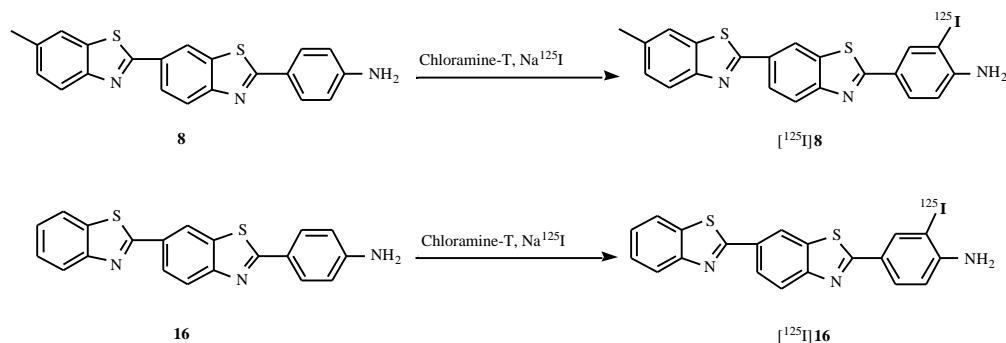
## 2.5. Brain Uptake of the Unlabeled Compounds

Based on quantitative binding assays using isolated human amyloid as well as postmortem AD tissue staining, the brain uptake of the unlabeled compound **17** was first evaluated. Following a single i.v. injection (0.4 ml of a solution containing saline (85%), DMSO (10%), HCl (5%, 0.3 nM)

and 1~2 mg **17**), the brain was removed and homogenized. HPLC analysis showed that brain uptake reached  $1.50 \pm 0.94\%$  ID as early as 5 minutes after injection. At 30 minutes, brain uptake increased to the peak level  $3.56 \pm 0.99$ , and then decreased gradually to  $2.80 \pm 0.87$  at 60 minutes post injection (Table 2).



**Scheme 3.** Radiosynthesis of [ $^{11}\text{C}$ ]17 through radiomethylation



**Scheme 4.** Radiosynthesis of [ $^{125}\text{I}$ ]8 and [ $^{125}\text{I}$ ]16 through electrophilic radioiodination.

**Table 2.** Brain uptake of unlabeled compound 17 in mice (n=3, %ID/g)

5 min	30 min	60 min
1.50 ± 0.94	3.56 ± 0.99	2.80 ± 0.87

Values are mean ± SD

## 2.6 Determination of Partition Coefficient

We radioiodinated **8** and **16** and used [ $^{125}\text{I}$ ]8 and [ $^{125}\text{I}$ ]16 to measure partition coefficients (logPoct), a parameter related to the lipophilicity of the compounds. Through conventional octanol-water partition methods, logPoct of [ $^{125}\text{I}$ ]8 and [ $^{125}\text{I}$ ]16 were determined at 3.10 and 2.70 respectively. The logPoct values of other ThS derivatives were then estimated based on coefficients determined by Hansch C and Leo A [49]. As shown in Table 1, the lipophilicity of these ThS derivatives are in the range of 1-3, high enough to penetrate BBB.

## 2.7. In Vivo Brain Uptake of [ $^{125}\text{I}$ ]8 and [ $^{125}\text{I}$ ]16

Encouraged by these results, we further evaluated the brain permeability of radiolabeled [ $^{125}\text{I}$ ]8 and [ $^{125}\text{I}$ ]16. The brain entry and clearance of [ $^{125}\text{I}$ ]8 and [ $^{125}\text{I}$ ]16 were determined in normal control mice. Following tail vein i.v. injection, the brain radioactivity concentration was determined at 2 min, 30 min, and 60 min. As shown in Table 3, both [ $^{125}\text{I}$ ]8 and [ $^{125}\text{I}$ ]16 readily penetrated the BBB, which is consistent

with the lipophilicity (3.05 for [ $^{125}\text{I}$ ]8 and 2.70 for [ $^{125}\text{I}$ ]16). [ $^{125}\text{I}$ ]8 and [ $^{125}\text{I}$ ]16 displayed rapid brain entry at early time points with  $1.82\% \pm 0.30\% \text{ID/g}$  and  $3.71\% \pm 0.63\% \text{ID/g}$  at 2 min, respectively. The brain radioactivity concentration decreased sharply to  $0.36 \pm 0.05\% \text{ID/g}$  and  $0.78 \pm 0.14\% \text{ID/g}$  at 30 min,  $0.37 \pm 0.07\% \text{ID/g}$  and  $0.43 \pm 0.12\% \text{ID/g}$  at 60 min, with a 2-to-30 min ratio of 5 (Table 3). These results indicate that both [ $^{125}\text{I}$ ]8 and [ $^{125}\text{I}$ ]16 could penetrate the BBB and rapidly clear from the normal mouse brain in the absence of amyloid deposits. The rapid clearance is desirable for low non-specific binding. The initial brain uptake of [ $^{125}\text{I}$ ]16 reached 3.71% ID/g, indicating a level sufficient for imaging brain. High brain uptake and rapid washout made [ $^{125}\text{I}$ ]16 a promising amyloid imaging agent.

## CONCLUSION

In summary, we reported here the design, synthesis, and evaluation of novel amyloid imaging probes based on the major component of ThS. These compounds selectively stain amyloid plaques and NFTs in postmortem AD brain with

**Table 3.** Brain Uptake in Mice (n=3, %ID/gram)

Compounds	2 min	30 min	60 min
[ $^{125}\text{I}$ ]16	3.71 ± 0.63	0.78 ± 0.14	0.43 ± 0.12
[ $^{125}\text{I}$ ]8	1.82 ± 0.30	0.36 ± 0.05	0.37 ± 0.07

Values are mean ± SD

high binding affinities for isolated AD human amyloid. One of these compounds, 2-(4'-methylaminophenyl)-6-(benzothiazolyl)benzothiazole (**17**), displayed higher affinity than that of PIB. In addition, *in vivo* biodistribution study of [<sup>125</sup>I]**16** in normal mice showed a good initial brain penetration and a fast washout from the brain. These studies suggested that novel ThS analogs, such as [<sup>11</sup>C]**17**, may be useful radiotracers for mapping amyloid plaques in the brain of AD subjects. Potential applications of these amyloid binding agents are under way to facilitate drug screening in animal models and use as *in vivo* markers of early and definitive diagnosis of AD.

## ACKNOWLEDGEMENTS

This work is supported in part by grants from the Alzheimer's Association, the Institute for the Study of Aging (YW) and the National Institute on Aging (AG22048, YM). This work is also supported by National Natural Science Foundation of P.R. China (30470496, CY, Wu) and Natural Science Foundation of Jiangsu Province, China (BK 2004-423, CY, Wu). We thank Rush Alzheimer's Disease Center for providing us with postmortem AD brain tissue sections. This work was partly supported by the Intramural Research Program of the National Institutes of Mental Health (NIMH).

## REFERENCE

- Katzman R. Education and the prevalence of dementia and Alzheimer's disease. *Neurology* 43:13-20 (1993).
- Olshansky SJ, Carnes BA and Cassel CK. The aging of the human species. *Sci Am* 268:46-52 (1993).
- Price DL and Sisodia SS. Mutant genes in familial Alzheimer's disease and transgenic models. *Annu Rev Neurosci* 21:479-505 (1998).
- Hardy JA and Higgins GA. Alzheimer's disease: the amyloid cascade hypothesis. *Science* 256:184-185 (1992).
- Hardy J and Selkoe DJ. The amyloid hypothesis of Alzheimer's disease: progress and problems on the road to therapeutics. *Science* 297:353-356 (2002).
- Braak H and Braak E. Evolution of neuronal changes in the course of Alzheimer's disease. *J Neural Transm Suppl* 53:127-140 (1998).
- Trojanowski JQ, Clark CM, Schmidt ML, Arnold SE and Lee VM. Strategies for improving the postmortem neuropathological diagnosis of Alzheimer's disease. *Neurobiol Aging* 18:S75-79 (1997).
- De Strooper B and Konig G. Alzheimer's disease. A firm base for drug development. *Nature* 402:471-472 (1999).
- Selkoe DJ. The origins of Alzheimer disease: a is for amyloid. *JAMA* 283:1615-1617 (2000).
- Roher AE, Lowenson JD, Clarke S, Wolkow C, Wang R, Cotter RJ. Structural alterations in the peptide backbone of beta-amyloid core protein may account for its deposition and stability in Alzheimer's disease. *J Biol Chem* 268:3072-3083 (1993).
- Citron M. Secretases as targets for the treatment of Alzheimer's disease. *Mol Med Today* 6:392-397 (2000).
- Hardy J, Duff K, Hardy KG, Perez-Tur J and Hutton M. Genetic dissection of Alzheimer's disease and related dementias: amyloid and its relationship to tau. *Nat Neurosci* 1:355-358 (1998).
- Selkoe DJ. Toward a comprehensive theory for Alzheimer's disease. Hypothesis: Alzheimer's disease is caused by the cerebral accumulation and cytotoxicity of amyloid beta-protein. *Ann N Y Acad Sci* 924:17-25 (2000).
- Naslund J, Haroutunian V, Mohs R, Davis KL, Davies P, Greenberg P. Correlation between elevated levels of amyloid beta-peptide in the brain and cognitive decline. *JAMA* 283:1571-1577 (2000).
- Wu CY, Pike VW and Wang YM. Amyloid Imaging - From Bench-top to Bedside. *Current Topics of Developmental Biology* in press:(2005).
- Mathis CA, Wang Y and Klunk WE. Imaging beta-amyloid plaques and neurofibrillary tangles in the aging human brain. *Curr Pharm Des* 10:1469-1492 (2004).
- Sair HI, Doraiswamy PM and Petrella JR. *In vivo* amyloid imaging in Alzheimer's disease. *Neuroradiology* 46:93-104 (2004).
- Nordberg A. PET imaging of amyloid in Alzheimer's disease. *Lancet Neurol* 3:519-527 (2004).
- Link CD, Johnson CJ, Fonte V, Paupard M, Hall DH, Styren S. Visualization of fibrillar amyloid deposits in living, transgenic *Caenorhabditis elegans* animals using the sensitive amyloid dye, X-34. *Neurobiol Aging* 22:217-226 (2001).
- Zhuang ZP, Kung MP, Hou C, Skovronsky DM, Gur TL, Plossl K. Radioiodinated styrylbenzenes and thioflavins as probes for amyloid aggregates. *J Med Chem* 44:1905-1914 (2001).
- Schmidt ML, Schuck T, Sheridan S, Kung MP, Kung H, Zhuang ZP. The fluorescent Congo red derivative, (*trans, trans*)-1-bromo-2,5-bis-(3-hydroxycarbonyl-4-hydroxy)styrylbenzene (BSB), labels diverse beta-pleated sheet structures in postmortem human neurodegenerative disease brains. *Am J Pathol* 159:937-943 (2001).
- Ishikawa K, Doh-ura K, Kudo Y, Nishida N, Murakami-Kubo I, Ando Y. Amyloid imaging probes are useful for detection of prion plaques and treatment of transmissible spongiform encephalopathies. *J Gen Virol* 85:1785-1790 (2004).
- Wang Y, Klunk WE, Huang GF, Debnath ML, Holt DP and Mathis CA. Synthesis and evaluation of 2-(3'-iodo-4'-aminophenyl)-6-hydroxybenzothiazole for *in vivo* quantitation of amyloid deposits in Alzheimer's disease. *J Mol Neurosci* 19:11-16 (2002).
- Klunk WE, Bacskaï BJ, Mathis CA, Kajdasz ST, McLellan ME, Frosch MP. Imaging Abeta plaques in living transgenic mice with multiphoton microscopy and methoxy-X04, a systemically administered Congo red derivative. *J Neuropathol Exp Neurol* 61:797-805 (2002).
- Styren SD, Hamilton RL, Styren GC and Klunk WE. X-34, a fluorescent derivative of Congo red: a novel histochemical stain for Alzheimer's disease pathology. *J Histochem Cytochem* 48:1223-1232 (2000).
- Okamura N, Suemoto T, Shimadzu H, Suzuki M, Shiomitsu T, Akatsu H. Styrylbenzoxazole derivatives for *in vivo* imaging of amyloid plaques in the brain. *J Neurosci* 24:2535-2541 (2004).
- Zhen W, Han H, Anguiano M, Lemere CA, Cho CG and Lansbury PT, Jr. Synthesis and amyloid binding properties of rhenium complexes: preliminary progress toward a reagent for SPECT imaging of Alzheimer's disease brain. *J Med Chem* 42:2805-2815 (1999).
- Dezutter NA, Dom RJ, de Groot TJ, Bormans GM and Verbruggen AM. <sup>99m</sup>Tc-MAMA-chrysin G, a probe for beta-amyloid protein of Alzheimer's disease. *Eur J Nucl Med* 26:1392-1399 (1999).
- Han H C, C. G., Lansbury, P. T. Jr. Technetium complexes for the quantitation of brain amyloid. *J Am Chem Soc* 118:4506-4507 (1996).
- Verhoeff NP, Wilson AA, Takeshita S, Trop L, Hussey D, Singh K. *In-vivo* imaging of Alzheimer disease beta-amyloid with [<sup>11</sup>C]SB-13 PET. *Am J Geriatr Psychiatry* 12:584-595 (2004).
- Ono M, Wilson A, Nobrega J, Westaway D, Verhoeff P, Zhuang ZP. <sup>11</sup>C-labeled stilbene derivatives as Abeta-aggregate-specific PET imaging agents for Alzheimer's disease. *Nucl Med Biol* 30:565-571 (2003).
- Kung HF, Lee CW, Zhuang ZP, Kung MP, Hou C and Plossl K. Novel stilbenes as probes for amyloid plaques. *J Am Chem Soc* 123:12740-12741 (2001).
- Wang Y, Mathis CA, Huang GF, Debnath ML, Holt DP, Shao L. Effects of lipophilicity on the affinity and nonspecific binding of iodinated benzothiazole derivatives. *J Mol Neurosci* 20:255-260 (2003).
- Klunk WE, Wang Y, Huang GF, Debnath ML, Holt DP and Mathis CA. Uncharged thioflavin-T derivatives bind to amyloid-beta protein with high affinity and readily enter the brain. *Life Sci* 69:1471-1484 (2001).
- Mathis CA, Wang Y, Holt DP, Huang GF, Debnath ML and Klunk WE. Synthesis and evaluation of <sup>11</sup>C-labeled 6-substituted 2-arylbenzothiazoles as amyloid imaging agents. *J Med Chem* 46:2740-2754 (2003).
- Cai L, Chin FT, Pike VW, Toyama H, Liow JS, Zoghbi SS. Synthesis and evaluation of two <sup>18</sup>F-labeled 6-iodo-2-(4'-N,N-dimethylamino)phenylimidazo[1,2-a]pyridine derivatives as prospective radioligands for beta-amyloid in Alzheimer's disease. *J Med Chem* 47:2208-2218 (2004).

- [37] Wang Y, Klunk WE, Debnath ML, Huang GF, Holt DP, Shao L. Development of a PET/SPECT agent for amyloid imaging in Alzheimer's disease. *J Mol Neurosci* 24:55-62 (2004).
- [38] Ono M, Kung MP, Hou C and Kung HF. Benzofuran derivatives as Abeta-aggregate-specific imaging agents for Alzheimer's disease. *Nucl Med Biol* 29:633-642 (2002).
- [39] Zhuang ZP, Kung MP, Wilson A, Lee CW, Plossl K, Hou C. Structure-activity relationship of imidazo[1,2-a]pyridines as ligands for detecting beta-amyloid plaques in the brain. *J Med Chem* 46:237-243 (2003).
- [40] Suemoto T, Okamura N, Shiomitsu T, Suzuki M, Shimadzu H, Akatsu H. *In vivo* labeling of amyloid with BF-108. *Neurosci Res* 48:65-74 (2004).
- [41] Shimadzu H, Suemoto T, Suzuki M, Shiomitsu T, Okamura N, Kudo Y. A novel probe for imaging amyloid- $\beta$ : Synthesis of F-18 labelled BF-108, an Acridine Orange analog. *J Label Compd Radiopharm* 46:765-772 (2003).
- [42] Lee CW, Kung MP, Hou C and Kung HF. Dimethylamino-fluorenes: ligands for detecting beta-amyloid plaques in the brain. *Nucl Med Biol* 30:573-580 (2003).
- [43] Agdeppa ED, Kepe V, Liu J, Flores-Torres S, Satyamurthy N, Petric A. Binding characteristics of radiofluorinated 6-dialkylamino-2-naphthylethylidene derivatives as positron emission tomography imaging probes for beta-amyloid plaques in Alzheimer's disease. *J Neurosci* 21:RC189 (2001).
- [44] Agdeppa ED, Kepe V, Petri A, Satyamurthy N, Liu J, Huang SC. *In vitro* detection of (S)-naproxen and ibuprofen binding to plaques in the Alzheimer's brain using the positron emission tomography molecular imaging probe 2-(1-[6-[(2-[(18F)fluoroethyl](methyl)amino]-2-naphthyl]ethylidene)malono nitrile. *Neuroscience* 117:723-730 (2003).
- [45] Jacobson A, Petric A, Hogenkamp D, Sinur A and Barrio JR. 1,1-Dicyano-2-[6-(dimethylamino)naphthalen-2-yl]propene (DDNP): A solvent polarity and viscosity sensitive fluorophore for fluorescence microscopy. *J Am Chem Soc* 118:5572-5579 (1996).
- [46] Wu C, Pike VW and Wang Y. Amyloid imaging: from benchtop to bedside. *Curr Top Dev Biol* 70:171-213 (2005).
- [47] Wei J, Wu C, Lankin D, Gulrati A, Valyi-Nagy T, Cochran E. Development of novel amyloid imaging agents based upon thioflavin S. *Curr Alzheimer Res* 2:109-114 (2005).
- [48] Schubert VM. Zur Kenntnis der dehydrothiolutidin- und primulin-sulfosaure. *Justus Liebigs Ann Chem* 558:10 (1947).
- [49] Hansch C and Leo A. substituent constants for correlation analysis in chemistry and biology. John Wiley & Sons, New York (1979).